

ARTICLE

Doublecortin mutations cluster in evolutionarily conserved functional domains

Tamar Sapir, David Horesh, Michal Caspi, Roe Atlas, Harold A. Burgess, Sharon Grayer Wolf¹, Fiona Francis¹, Jamel Chelly³, Michael Elbaum², Shmuel Pietrokovski and Orly Reiner[†]

Department of Molecular Genetics, ¹Electron Microscopy Unit and ²Department of Materials and Interfaces, The Weizmann Institute of Science, 76100 Rehovot, Israel and ³Institut Cochin de Genetique Moleculaire, INSERM U129, CHU Cochin-Port-Royal, 24 rue du Faubourg Saint-Jacques, 75014 Paris, France

Received 29 November 1999; Revised and Accepted 25 January 2000

Mutations in the X-linked gene *doublecortin* (*DCX*) result in lissencephaly in males or subcortical laminar heterotopia ('double cortex') in females. Various types of mutation were identified and the sequence differences included nonsense, splice site and missense mutations throughout the gene. Recently, we and others have demonstrated that *DCX* interacts and stabilizes microtubules. Here, we performed a detailed sequence analysis of *DCX* and *DCX*-like proteins from various organisms and defined an evolutionarily conserved Doublecortin (DC) domain. The domain typically appears in the N-terminus of proteins and consists of two tandemly repeated 80 amino acid regions. In the large majority of patients, missense mutations in *DCX* fall within the conserved regions. We hypothesized that these repeats may be important for microtubule binding. We expressed *DCX* or *DCLK* (KIAA0369) repeats *in vitro* and *in vivo*. Our results suggest that the first repeat binds tubulin but not microtubules and enhances microtubule polymerization. To study the functional consequences of *DCX* mutations, we overexpressed seven of the reported mutations in COS7 cells and examined their effect on the microtubule cytoskeleton. The results demonstrate that some of the mutations disrupt microtubules. The most severe effect was observed with a tyrosine to histidine mutation at amino acid 125 (Y125H). Produced as a recombinant protein, this mutation disrupts microtubules *in vitro* at high molar concentration. The positions of the different mutations are discussed according to the evolutionarily defined DC-repeat motif. The results from this study emphasize the importance of *DCX*-microtubule interaction during normal and abnormal brain development.

INTRODUCTION

The lissencephaly syndromes in humans involve abnormal cortical lamination and are medically categorized as neuronal migration defects (1,2). The various human lissencephalies are classified according to morphology or putative etiology (3,4). Two types of lissencephaly have been defined (5,6). In type I, also known as classical lissencephaly, the cortex consists of four layers instead of the normal six, whereas in type II, also known as cobblestone lissencephaly the cortex is unlayered (4). Two lissencephaly type I disease genes have been identified. The first lissencephaly gene cloned was *LIS1* (7) (recently reviewed in ref. 8). Mutations in one allele of this gene (7,9) are sufficient to cause lissencephaly type I. *LIS1* interacts with tubulin and influences microtubule dynamics (10). It has also been cloned independently as a non-catalytic subunit of platelet-activating factor acetylhydrolase (11). A second lissencephaly type I gene was mapped to the X

chromosome (12,13). It was cloned and termed *doublecortin* (*DCX*) (14,15). Mutations in the X-linked *DCX* gene result in lissencephaly in males or subcortical laminar heterotopia (SCLH), i.e. 'double cortex', in females (14,15).

It has been hypothesized that due to random X-inactivation, affected females heterozygous for the X-linked mutation show a milder phenotype, though so far this has not been conclusively shown and other mechanisms may also be involved. The milder phenotype consists of a brain with bilateral plates or bands of gray matter located beneath the cortex and ventricle but separated from both, hence the descriptive term double cortex, also known as SCLH (16). The clinical severity of SCLH varies strikingly from asymptomatic clinical presentation with heterotopic bands assessed by magnetic resonance imaging, to severe mental impairment with intractable epilepsy. The relative thickness of the heterotopic band seems to correlate with the phenotype, as

[†]To whom correspondence should be addressed. Tel: +972 8 9342319; Fax: +972 8 9344108; Email: lvreiner@wicc.weizmann.ac.il

patients with thicker bands have more severe mental retardation and seizures (17). To date, 39 various mutations were identified resulting in nonsense, splice site and missense mutations throughout the gene (14,15,18–21). Recently mutations both in *LIS1* and *DCX* that result in SCLH in male patients have been reported (22). No clear correlation was observed between the clinical severity and mutation profiles (18). However, it has been noticed that amino acid substitution mutations were much more common in inherited lissencephaly (19). Single amino acid substitution mutations (19 described so far) in *DCX* cluster in two regions: amino acids 43–125 and 178–253 (19). Among these 19 amino acids, two have been independently substituted to different amino acids: tyrosine 125 to histidine or aspartic acid, and isoleucine 250 to threonine or asparagine. Initially, the sequence of *DCX* revealed similarity to a cDNA from human brain (KIAA0369) (23). The deduced amino acid sequence of human KIAA0369 protein contains two domains: an N-terminal segment similar to Doublecortin (85% similarity) and a C-terminal domain nearly identical to the previously discovered kinase CPG16 in rat (24–27). Therefore, we suggested naming this protein Doublecortin-like kinase (DCLK) (28). Human KIAA0369 cDNA has been sequenced and mapped to human chromosome 13q12.3 (29,30). So far no neurological disorders have been mapped to this region. Recently, we and others have defined the first function for *DCX* as a microtubule-associated protein that stabilizes microtubules (31–33). Our results demonstrated that the first 213 amino acids of *DCX* are sufficient to bind microtubules, whereas the region from amino acid 110 to the C-terminus did not (33).

In order to gain further insight on protein function, we performed an advanced computer analysis of proteins with DC-like domains from vertebrates, insects, worms and fungi. The analysis identified an 80 amino acid region that typically appears as two repeats in the N-termini of the proteins. In order to study the function of the repeats we have expressed each of the DC-domain repeats and both of them (including an intervening sequence) *in vitro* and *in vivo*. To study the functional consequences of *DCX* mutations, we overexpressed seven of the reported mutations in *DCX* (14,15) in COS-7 cells. Overexpression of several of the mutations resulted in bundling of microtubules similar to the wild-type protein. However, some of the mutated proteins aggregated in the cells and disrupted the microtubule cytoskeleton. Mutation Y125H had the most striking phenotype when overexpressed and was further subjected to *in vitro* analysis. In this paper, we define the DC domain region and its conserved motifs in various organisms and proteins and show that *DCX* mutations can result in different functional consequences. We discuss our experimental results in the context of the conserved domains.

RESULTS

Conserved domains in *DCX*

Database searches with *DCX* and *DCLK* (28) (also known as KIAA0369) identified a number of other proteins with the DC domain (Fig. 1A). Some of these were only available as EST fragments and probably represent partial gene sequences. The domain was found in genes from human, mouse, rat, *Caenorhabditis elegans*, *Drosophila* and *Dictyostelium*. The

human and some of the *C.elegans* sequences were previously reported (34). However, we could not confirm the presence of a DC domain in a *Schizosaccharomyces pombe* protein reported in that work.

A multiple alignment analysis of the protein sequences identified a conserved region of ~80 amino acids that appears in one or two tandemly repeated copies in the N-terminal ends of the proteins. Vertebrate *DCX* and *DCLK* (28), also known as KIAA0369 (23), *ORP1* from human and mouse (34), a *C.elegans* homolog of *DCLK* and the *Dictyostelium* protein all have two copies of the region separated by 40–95 amino acids (Fig. 1A). In this work, we designated the first part of human *DCX* as pep1, the second as pep2 and both including intervening sequences as pep(1+2) (Fig. 1A and B). It is possible that the other proteins are of partial sequence and also have a second DC region. The position of the 19 reported lissencephaly-causing amino acid substitution mutations described so far (14,15,18–22) are indicated on the sequence (Fig. 1B), and the large majority (17 in total) fall within the designated region. All 15 repeats shown in Figure 1A were used for multiple sequence alignment. The DC region consists of four ungapped conserved motifs (A–D, where their positions within the sequence of *DCX* are indicated in Fig. 1B) that can be confidently aligned. It is clear that some amino acid residues are more conserved than others (Fig. 1C), for example amino acids 8–11 in the A domain are in most repeats RNGD.

Expression of repeated domains

In vitro. Computational sequence analysis of the human *DCX* protein identified in it a DC domain made up of a region repeated in amino acids 52–133 and 179–257. We expressed them as glutathione *S*-transferase (GST) fusion recombinant proteins: pep1 (amino acids 51–135), pep2 (amino acids 178–259) and pep(1+2) (amino acids 51–259) (Fig. 1B). We examined whether the peptides have the capability of binding to pre-assembled microtubules as shown previously with the full-length protein *DCX* (33). As can be seen in Figure 2A, pep1 and pep2 did not bind to pre-assembled microtubules; however, pep(1+2) is found both in the soluble and in the insoluble pellet bound to microtubules. Treatment with nocodazole resulted in complete solubilization of the pellet fraction of pep(1+2) (Fig. 2A). Next, we examined whether the peptides interact with tubulin subunits. In a pull-down assay using brain extract, pep1 and pep(1+2) pulled down a significant amount of tubulin, whereas pep2 pulled down less tubulin (Fig. 2B). However, the results obtained using purified tubulin demonstrated that only pep(1+2) pulled down a significant amount of tubulin (Fig. 2C). This assay was performed under conditions that do not support microtubule assembly (cold incubation and low protein concentration). The different results in these assays using pep1 may suggest that this peptide is able to recruit additional protein(s) from brain extract that facilitate the interaction with tubulin.

In order to examine whether the peptides may affect microtubule formation, we measured the assembly rate of tubulin using a light-scattering assay (Fig. 3). This assay is based on an increase in optical scattering as microtubules polymerize, measured as an effective optical density. Addition of pep1 or pep(1+2) to tubulin without *DCX* increased the assembly rate of tubulin (Fig. 3). Addition of pep2 by itself to

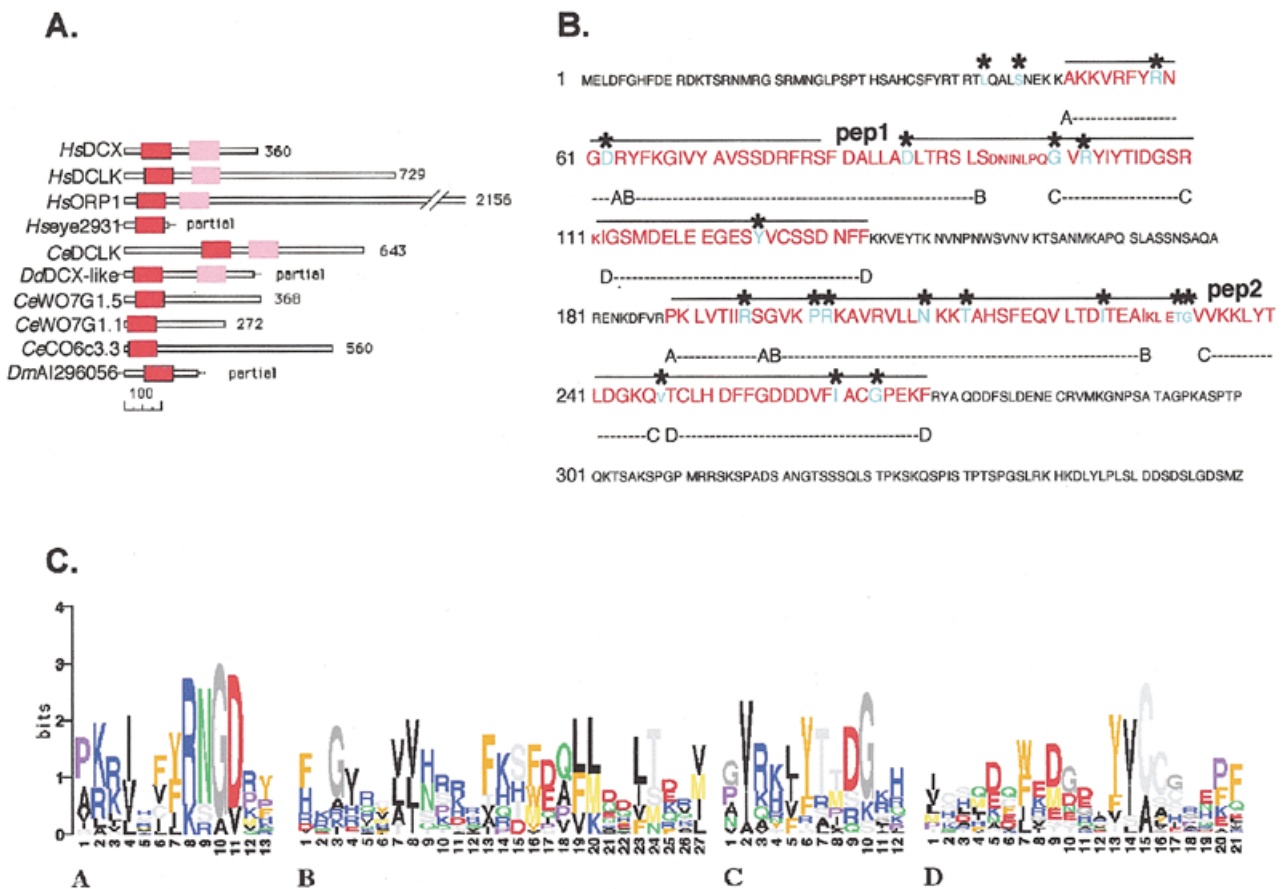


Figure 1. (A) Proteins with the doublecortin domain. Schematic representation of protein sequences found to have doublecortin domain(s). The domain is boxed on the line showing the protein sequence, the first domains are colored in red and the second in pink. Sequence names are shown on the left and length of the proteins on the right. Sequence lengths and scale bar are in amino acids. Species designations: Hs, human; Ce, *C. elegans*; Dd, *Dictyostelium discoideum* (slime mold); Dm, *Drosophila melanogaster*. NCBI sequence accession numbers are: Hs DCX, 2739176; Hs DCLK, 2224679; Hs ORP1, 5326860; Hs eye2931, 1553161 + 1552091 + 01064654 + 943176; Ce DCLK, 5824876; Dd DCX-like, 5162175 + 4881956 + 3799527 + 3219069 + 3073998 + 3060945 + 3984067; Ce W07G1.5, 4008399; Ce W07G1.1, 4008395; Ce C06C3.3, 3873997; Dm AI296056, 3945463. (B) Amino acid sequence of DCX. The positions of pep1 and pep2 are marked by a line above, and the relevant amino acids are red. The amino acids that are mutated in patients are colored in turquoise and marked above by an asterisk (*). The internal A–D subdomains are shown by dashed lines below the sequence. (C) Conserved sequence motifs in doublecortin domain. Motifs are designated A–D, their position in the sequence of human DCX is indicated in (B). Multiple alignments of the motifs from the doublecortin domains in (A) are shown as sequence logos (52,64). The height of each amino acid represents bits of information and is proportional to its conservation at that position (y-axis), after the sequences have been weighted and frequencies adjusted by the expected amino acid frequency. Below the logos is the numbering of amino acids within the internal A–D subdomains.

tubulin had the lowest effect on increase of the assembly (Fig. 3 and data not shown). Addition of pep1 or pep(1+2) to DCX and tubulin had an additive effect on microtubule assembly whereas pep2 reduced the effect of the normal protein. Previously, we have shown that addition of DCX to tubulin resulted in microtubule bundling (33). We examined the effect of the peptides on microtubule bundling effect by electron microscopy. In the presence of pep(1+2) microtubule bundles were formed (Fig. 4, compare A with B). We could not assess bundling activity of the individual repeat units (pep1 or pep2; data not shown).

In vivo. The three peptides composed of pep1, pep2 and pep(1+2) of DCLK were expressed transiently in COS-7 cells using PECE-FLAG expression vector. Similar to the *in vitro* experiments that were done with DC repeats, pep1 and pep2 did not bind microtubules in cells. However, pep(1+2) did bind microtubules to some extent. We used the well established protocol of gentle cell extraction with non-ionic detergent (0.5% Triton X-100) that

removes lipids and soluble proteins, leaving intact the detergent-insoluble matrix composed of the nucleus, the cytoskeleton framework and cytoskeleton-associated proteins. Gentle detergent extraction showed that the pep1 and pep2 were in the soluble fraction (Fig. 5A); however, pep(1+2) was also in the insoluble fraction (Fig. 5A, two right lanes). Immunostaining of cells confirmed the biochemical fractionation and, although the immunostaining of pep1 or pep2 seems cytoplasmic, immunostaining of pep(1+2) reveals staining of cytoskeletal structures resembling microtubules (Fig. 5B–D). This cytoskeletal staining was not completely identical with staining of cells transfected with the full-length DCLK (Fig. 5E), as the fibers appear thinner. Nevertheless, pep(1+2) cytoskeletal staining was disrupted by nocodazole treatment (Fig. 5F) that disrupts microtubule staining (Fig. 5G).

Mutated DCX expression in COS cells

In order to define the intracellular localization of mutated DCX, we transiently transfected COS-7 epithelial cells with

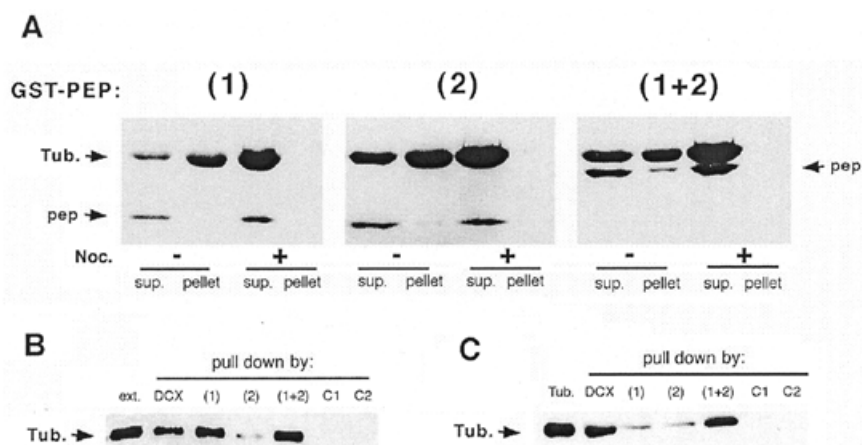


Figure 2. (A) Binding of GST-peptides to pre-assembled microtubules. Microtubules were pre-assembled from purified tubulin in PEM buffer. Polymerization was done with (+) and without (-) nocodazole (Noc.). GST-PEP1 (1), -PEP2 (2), and -PEP(1+2) (1+2) were added after polymerization and incubated with the microtubules for 10 min at 37°C. Assembled microtubules and associated proteins (pellet) were sedimented by centrifugation. Pellets and supernatants (sup.) were run on SDS-PAGE gels and stained with Coomassie blue. (B and C) Pull-down by GST-peptides. Brain extract (500 µg) (B) or purified tubulin (10 µg) (C) were incubated with 10 µg of GST-DCX (DCX), -PEP1 (1), -PEP2 (2), -PEP(1+2) (1+2) and GST as control. The pull-down assay was performed as described. ext., 50 µg of brain extract (B); Tub., 2 µg of tubulin (C); C1, GST control; C2, beads control. Note the difference in the amount of tubulin that was pulled down by GST-PEP1 between brain extract and pure tubulin.

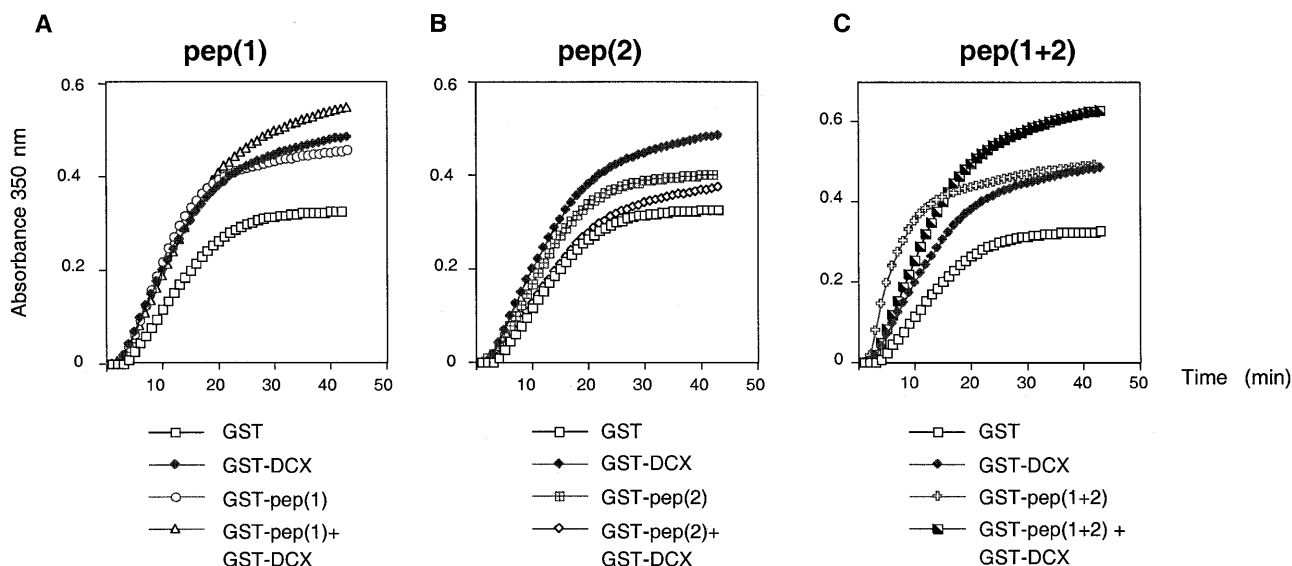


Figure 3. DCX peptides affect tubulin assembly rate *in vitro*. The assembly rate of tubulin was measured using a light-scattering assay. The concentration of tubulin used was 25 µM. The optical absorbance was recorded every minute for 40 min. The recombinant proteins used were GST, GST-DCX, -pep(1), -pep(2) and -pep(1+2) each at a final concentration of 4 µM. The recombinant proteins were added prior to the measurement. When indicated, two proteins were added together each at a concentration of 4 µM. Both pep(1) (A) and pep(1+2) (C) increased the assembly rate of tubulin to one similar to that for adding the full-length DCX. When the pep1 or pep(1+2) were added together with DCX the assembly rate increased beyond that of each protein alone (A and C). In the presence of pep(2), a small increase in the assembly rate was observed (B). When added to DCX the assembly rates were reduced back to the basal levels, suggesting that pep(2) interfered with DCX function.

FLAG-tagged DCX constructs. For this analysis we used seven mutations (15,18). All the DCX mutated proteins were readily expressed in COS-7 cells demonstrated by western blot analysis (Fig. 6). Biochemical fractionation of exogenous expressed protein did not suggest any significant difference between the mutated DCX and normal DCX. In transfected COS-7 cells, the exogenous DCX (recognized by FLAG tag) appeared mainly in the detergent-insoluble fraction (Fig. 6).

One of the key questions in understanding the function of DCX concerns its intracellular localization. Our previous

analysis demonstrated that DCX colocalizes with the microtubule cytoskeleton and stabilizes the polymerized microtubules. Immunostaining of transfected COS-7 cells allowed assaying for, and to distinguish between, different effects of the DCX mutations. Overexpression of mutation R192W did not change cell morphology and this mutated DCX colocalized with microtubules (data not shown). Another group of DCX mutations (T203R, R59L, S47R) where the overexpressed protein colocalized to microtubules caused microtubule bundling and cell morphology was changed (Fig.

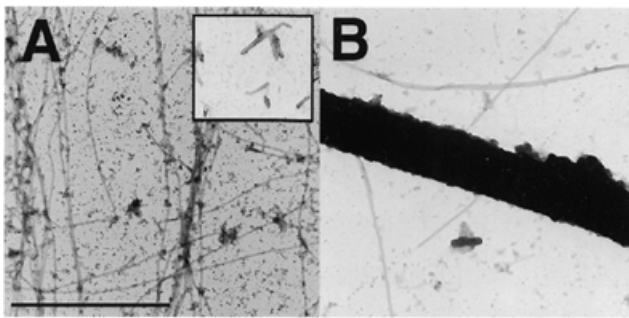


Figure 4. Electron microscopy analysis of microtubules in the presence of pep(1+2) PC-tubulin (22 μ M) was incubated in the presence of GST or GST-pep(1+2) (15 μ M) for 30 min at 37°C. Samples were loaded onto a grid, stained with uranyl acetate and examined by electron microscopy. The magnification used is $\times 10\,000$; bar, 2.5 μ m. Most microtubules in the control sample (tubulin and GST) appeared as individual microtubules (A). Small aggregates of microtubules were sometimes observed [small box in (A)]. In the presence of pep(1+2), large bundles were observed (B).

7). This is the general effect previously observed with overexpression of the wild-type DCX protein. The change in cell morphology can be appreciated when looking at two cells stained with anti-tubulin antibodies in Figure 7b. The transfected cell (compare with Fig. 7a) is considerably smaller and the microtubules are clearly bundled in comparison with the well spread untransfected cells with a nicely developed cytoskeleton. The microtubules in the cells transfected with these mutations (T203R, R59L, S47R) are stable as determined by staining with anti-acetylated-tubulin antibodies (Fig. 7e, h and i). The overall cellular structure of overexpression of this group of mutated DCX proteins revealed a very similar pattern as overexpressing the wild-type protein; i.e. colocalization with the microtubule cytoskeleton as observed by immunostaining (Fig. 7c, f, i and l).

The last group of DCX mutated proteins appeared aggregated in COS-7 cells, and did not convincingly colocalize with microtubules (D246X, Y125H, D62N) (Fig. 8). The morphology of these cells was affected, and most of the cells appeared smaller. Microtubules of these cells seemed to be disrupted especially where mutated DCX aggregates appeared. In the case of mutation D246X and D62N, high levels of overexpression resulted in different cell morphology. However, in cells with relatively low levels of overexpression, the microtubule cytoskeleton was not significantly disturbed (data not shown). Mutation Y125H was the most severe mutation, and the morphology of most of the cells changed. Therefore, we decided to investigate the effects of this mutation using *in vitro* studies.

Recombinant Y125H protein and microtubules

Our *in vivo* experiments suggested that the levels of overexpression as well as the type of the mutation expressed determine the effect on the cell cytoskeleton. To study how different concentrations of mutated DCX (Y125H) affect tubulin polymerization, we used differential interference contrast (DIC) microscopy. Enhancement of microtubule assembly on introduction of low concentration of Y125H was observed (Fig. 9). When the concentrations of Y125H were equal to or higher than the tubulin concentration the picture

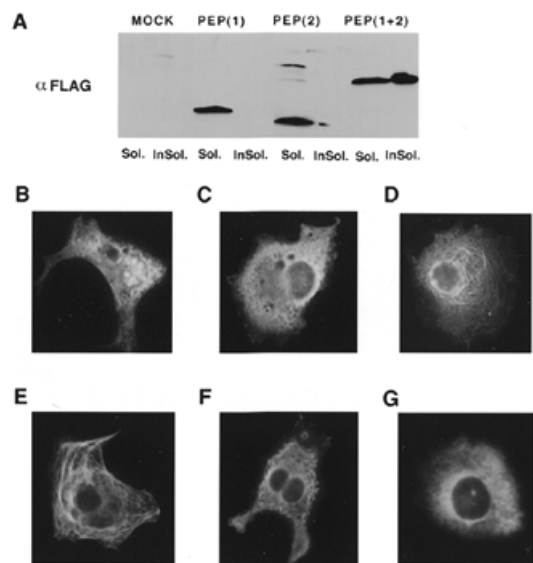


Figure 5. (A) Detergent extraction assay with DCLK peptides. 293 cells were transfected with PECE-FLAG-PEP1, PEP2, PEP(1+2) and GFP control. Detergent assay was performed as described in Materials and Methods. It can be clearly observed that whereas PEP1 and PEP2 are restricted to the soluble fraction of the cells, PEP(1+2) is distributed to both the soluble (Sol.) and insoluble (InSol.) fractions. MOCK, GFP-transfected cells. (B–G) Localization of the different DCLK peptides: COS-7 cells were transfected with PECE-FLAG constructs containing DCLK, DCLK-PEP1, PEP2 and PEP(1+2). The cells were stained with α -FLAG antibodies (B–F) or α -tubulin (G). (B) PEP1; (C) PEP2; (D) PEP(1+2); (E) DCLK; (F) PEP(1+2) after nocodazole treatment; (G) tubulin cytoskeleton disrupted by nocodazole treatment as seen in α -tubulin staining. Mutated DCX proteins were detected mainly in the detergent insoluble fractions.

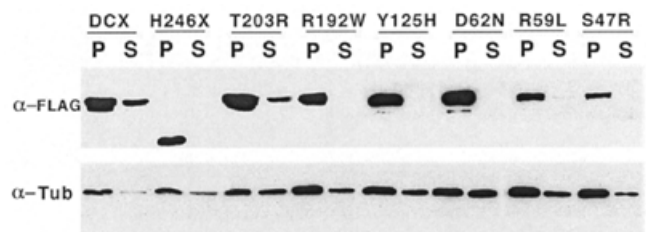


Figure 6. Exogenous DCX and DCX mutated proteins appear in detergent-insoluble cellular fractions. COS-7 cells were transfected with FLAG-DCX and mutated FLAG-DCX. Transfected cells were harvested 48–72 h after transfection and subjected to detergent extraction as described in Materials and Methods. Equal amounts (10 μ g) of soluble (S) and insoluble (P) fraction were separated on SDS-PAGE, immunoblotted and reacted with anti-FLAG antibodies (top) and anti-tubulin antibodies (bottom). Normal as well as mutated DCX proteins were detected mainly in the detergent-insoluble fraction.

completely changed. The protein formed aggregates and the filaments of microtubules were disrupted (Fig. 9). Taking into consideration the disrupted microtubule cytoskeleton in cells overexpressing this mutation and the fact that these aggregates did not appear in the absence of tubulin (Fig. 9), we assume that the aggregates result from microtubule severing.

DISCUSSION

Many different mutations occur in the *DCX* gene and all of them can result in SCLH. Point mutations are most common in

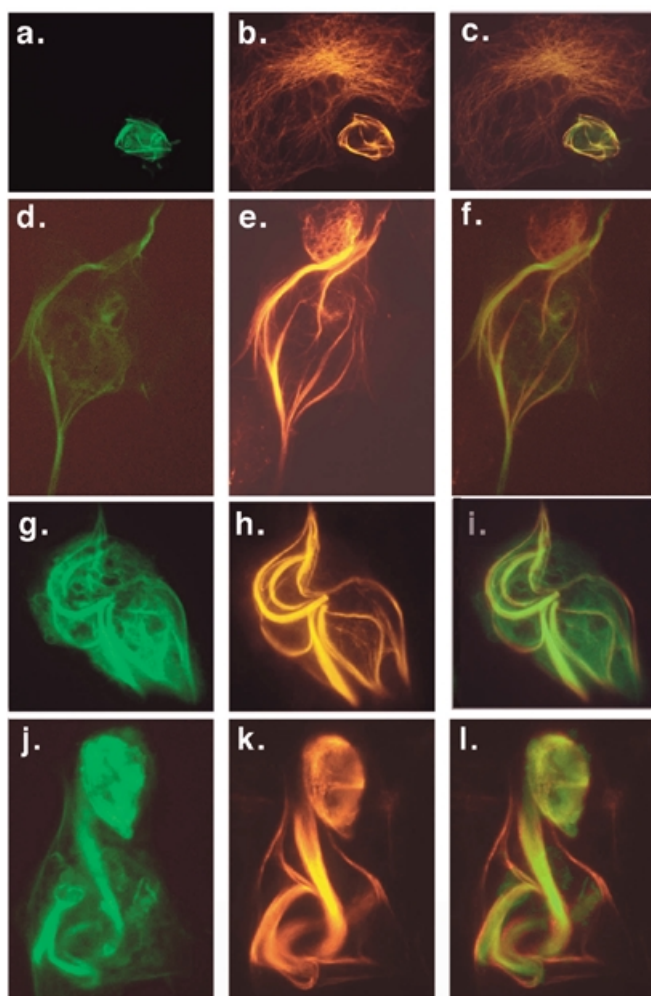


Figure 7. Overexpression of DCX mutations R59L, T203R and S47R in COS-7 cells. COS-7 cells were transfected with FLAG-DCX mutations; 48 h after transfections, cells were fixed with cold methanol double-stained with anti-Doublecortin primary antibodies and secondary anti-rabbit-FITC (a, d, g and j), and anti- α -tubulin antibodies secondary anti-mouse rhodamine (b), or anti-acetylated-tubulin antibodies secondary anti-mouse rhodamine (e, h and k). The colocalization is demonstrated by computer-derived overlap (c, f, i and l). Cells were transfected with DCX mutation R59L (a-f), T203R (g-i) and mutation S47R (j-l).

males with lissencephaly (14,15,18–21). Rare cases with missense mutations in DCX or LIS1 that result in SCLH have been described recently (22). Our results suggest that different mutations can yield different functional disturbances and result in either SCLH or lissencephaly. Our analysis focused mainly on missense mutations, although one (D246X) was a truncation mutation. Interestingly, the large majority of point mutations cluster within the conserved DC motifs that we have defined. The multi-alignment analysis performed reveal that some of the missense mutations are dramatic and are likely to disturb protein function. For example the eighth amino acid of pep1 and pep2 is highly conserved among species and is either arginine or lysine in all the DC domains known to date. In DCX there is an arginine in this position and there are lissencephaly-causing mutations both in the first (R59L) and second (R186C) repeats. Other mutations may be considered to be less severe, in some cases the amino acid substitution is a

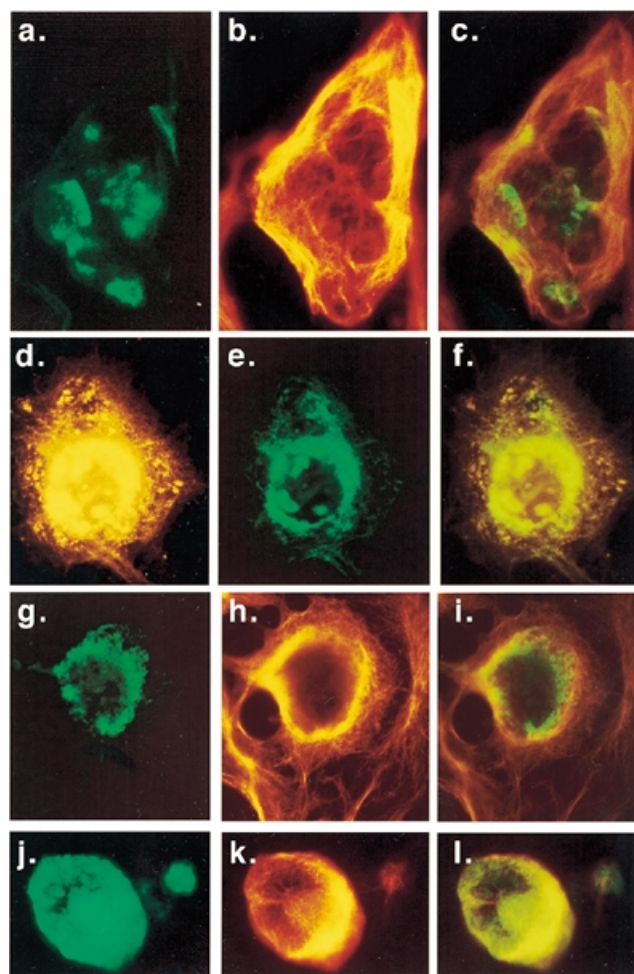


Figure 8. Overexpression of DCX mutations D246X, D62N, Y125H in COS-7 cells. COS-7 cells were transfected with FLAG-DCX mutations; 48 h after transfections, cells were fixed with cold methanol double-stained with anti-Doublecortin primary antibodies and secondary anti-rabbit-FITC (a, g and j) or secondary anti-rabbit rhodamine (d), and anti- α -tubulin antibodies secondary anti-mouse rhodamine (b and h) or secondary anti-mouse-FITC (e), or anti-acetylated-tubulin antibodies secondary anti-mouse rhodamine (k). Computer-derived overlaps are also shown (c, f, i and l). Cells were transfected with DCX mutation D246X (a-c), D62N (d-f), Y125H (g-i).

conserved change that naturally occurs in other repeats (for example, T203R where R is found in the same position in the first repeat). Our experimental results suggest that pep1 and pep2 are not identical. Furthermore, comparing the repeats as independent units, it is apparent that the order of the repeats is important and the first repeats from several genes are more similar to each other than to the second repeats (data not shown). Thus, it is likely that a duplication leading to the DC domain repeat structure occurred before the divergence of the different genes containing tandemly repeats of DC domains. We speculate that the function of the repeats is conserved in evolution, though this hypothesis remains to be tested in a more rigorous fashion. Nevertheless, the results shown here demonstrate some similarities between DCX and DCLK. The first DC repeat, pep1, binds tubulin more strongly and increases tubulin polymerization as measured by optical density. Addition of the first repeat with DCX to tubulin

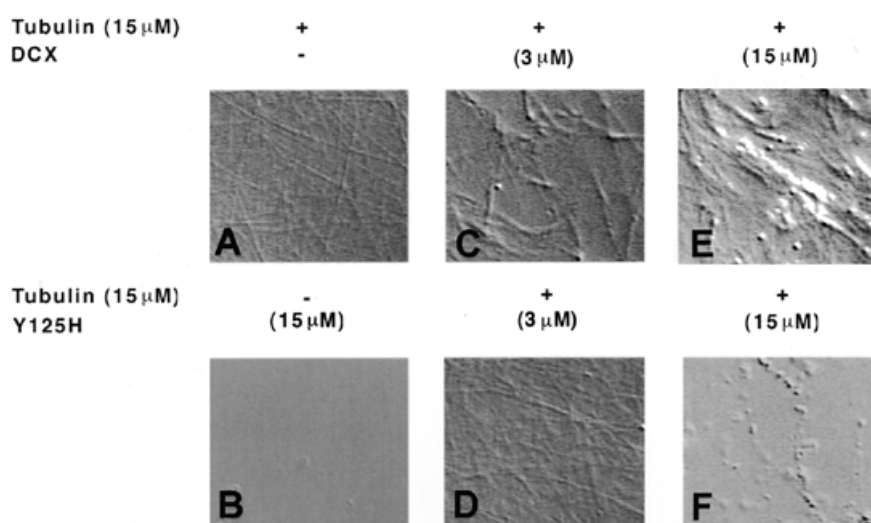


Figure 9. Severing of microtubules *in vitro* by high concentrations of DC Y125H. Equal concentrations of PC-tubulin (15 μM) were incubated at 30°C in the absence or presence of DCX or DCX Y125H. Microtubules were visualized by DIC microscopy. Hardly any spontaneous polymerization was observed (A). Normal DCX enhanced microtubule assembly at lower molar ratios [DCX:tubulin 1:5, (E)] and caused bundling at higher concentration [DCX:tubulin 1:1 (C)]. When high concentrations of DCX Y125H were present no bundles were observed and instead large aggregates appeared [DCX Y125H:tubulin 1:1 (D)]. This effect was less severe when DCX Y125H concentrations were reduced and some fibers were observed [DCX Y125H:tubulin 1:5, (F)]. No aggregate protein was seen in samples lacking tubulin, which contain high concentrations of recombinant DCX Y125H (B).

increased the assembly rate whereas addition of the second repeat decreased the assembly rate. It has been shown that charge is important in tubulin and microtubule-associated protein interactions. However, the differences between DCX pep1 and pep2 cannot be explained by difference in charge. There is no obvious difference in the isoelectric points: the pI of pep1 is 9.23 and the pI of the pep2 is 10.16, the pI of the DC motif including the intervening sequence is 10.24.

There are several striking similarities between DCX and Tau. Tau is a neuronal microtubule-associated protein that promotes microtubule assembly and bundling in axons (35–37). Tau contains three to four tandem repeats, and the repeat domain enhances microtubule assembly. *In vitro* studies using peptides from the repeat domain showed binding and assembly activity especially by the first repeat but with much lower affinities than the intact protein (38,39). In a similar fashion DC repeat motifs do not mimic all DCX–microtubule-related activity. Only when both repeats are expressed do they partly localize to microtubules *in vivo*, partly bind to pre-assembled microtubules *in vitro* and cause bundling of microtubules. Studies of the tau protein revealed that the inter-repeat region also has microtubule-binding capacity (40) and regions flanking the microtubule-binding domain play important regulatory roles in enhancing the binding affinity of the repeats (41–43). The results obtained in this study and our previous results (33) suggest that the DCX N-terminal region (amino acids 1–52) is important for the interaction with microtubules. This may be a direct or indirect effect, as this region may also bind the microtubule itself or may simply be involved in proper folding of the whole DCX protein, respectively. Naturally occurring lissencephaly-causing mutations also suggest the importance of this region, as there are lissencephaly-causing missense mutations in the first 52 amino acids. The variability seen in our system indicates that there is more than one way to alter the function of the DCX protein; disruption of microtubules is probably one of them. This is not the case with disease-causing mutations in tau. These mutations which result in inherited dementia typically involve one of the microtubule-binding

domains of Tau (44). The mutated tau protein products have weaker binding to microtubules (45,46). In a similar fashion, functional characterization of mutations found in the *MIDI* gene, which is mutated in Opitz syndrome (multiple congenital anomaly involving midline structures, developmental delay and mental retardation), revealed that association with microtubules is compromised (47,48).

The outcome of DCX mutations is clearly more variable, there are mutations that may have less or equal microtubule-bundling activity, some may have higher activity, and the most dramatic may disrupt microtubules altogether. Microtubule disruption quite similar to the effect seen with the DCX mutation Y125H was seen with overexpression of MARK protein kinases that phosphorylate microtubule-associated proteins (49). The site of this mutation (Y125H) may interfere in phosphorylation of the predicted Abl phosphorylation site (Y70). The variability seen in our experiments suggests the existence of additional functions for DCX that are not yet discovered.

We have defined here a new evolutionarily conserved motif that may be functionally conserved as well. Most disease-associated point mutations cluster in this region. We have found that this region is involved in DCX–microtubule function, therefore indirectly implying that DCX–microtubule function is important during brain development. Understanding the outcome of DCX mutations will expand the knowledge about the pathophysiology of lissencephaly and processes that are important during normal brain development.

MATERIALS AND METHODS

Computational sequence analysis

Sequences were retrieved from the NCBI and Sanger Centre databases. Database searches were performed on these databases with the BLAST program (50,51). Local multiple alignment was done using the BlockMaker (52) and MACAW

(53) programs as previously described (54,55). Although no alignment position is absolutely conserved, the resulting blocks were significantly sensitive and selective in distinguishing proteins with DC domains from all other proteins. Searching the SwissProt database release 37 (78 000 sequences) augmented with 14 DC domain proteins with the DC blocks using the BLIMPS (52) program gave perfect and almost perfect (12/14) separation of the true positives and true negatives, giving equivalence values (56) of 0 and 2 and receiver operating curves (57) of 1 and 0.999.

Cell culture

COS-7 cells (58) were grown at 37°C with 5% CO₂ and 95% air in Dulbecco's modified Eagle's medium supplemented with 10% fetal bovine serum, 4 mM glutamine, 100 U/ml penicillin and 0.1 mg/ml streptomycin. Cultures were split using standard trypsinization procedures. COS-7 cells were transfected using DEAE transfection procedure (59) with 20 µg of DNA in the absence of serum in the media. Four hours after transfection the media was aspirated and 10% DMSO was added for 2 min. The cells were washed and fresh standard growth media added. Transfected cells were then analyzed at various times for expression of exogenous protein. Efficiency of transfections was estimated using a green fluorescent protein (GFP) expression vector (Clontech, Palo Alto, CA).

Plasmid construction

Wild-type DCX was cloned in the pRSET vector (Qiagen, Hilden, Germany), using two *EcoRI* sites and single-strand DNA was prepared. The mutations were introduced using site-directed mutagenesis (59). The oligonucleotides used were: D246X, 5'-gactcggcattctgtttccatc-3', T→R amino acid 203; 5'-gagtgggctCtctctgttgc-3', R→W amino acid 192; 5'-cagcctccAaggtctacc-3', Y→H amino acid 125; 5'-ctgaggaacaCACGTGgcttcccc-3', D→N amino acid 62; 5'-gaagtagcggfTcccattgcg-3', R→L amino acid 59; 5'-gtccccattgAggtagaaacg-3', S to R amino acid 47; 5'-cttctcattacGcagtgccg-3'.

All of the mutations were verified by sequencing. The *EcoRI* fragments containing the mutated DCX coding regions were then cloned into pECE (60) with the FLAG epitope at their N-terminus.

DC repeats from DCX and DCLK (28) were cloned using PCR with the following primers:

Pep1 mouse DCLK, 5'-cgGaattcAAAGCCAAGAAGGTTTC-3';
 Pep2 mouse Pep1 mouse DCLK, 5'-cgGaattcAAAGCCAAGAAGGTTTC-3';
 Pep2 mouse DCLK, 5'-CgGaattcCGACCCAAGCTGGTC-3';
 PEP1 DCX, 5'-cgGaattcAAAGCCAAGAAGGTAC-3';
 PEP2 DCX, 5'-cgGAATTCCGCCCAAGCTGGTTAC-3';
 PEP1 Mouse 3' DCLK, 5'-CGTCTAGATCACTTAAAGGGCTCGAT-3';
 PEP2 Mouse 3' DCLK, 5'-CGTCTAGATCAACGGAAGTCTCTGG-3';
 PEP1 3' DCX, 5'-CGTCTAGATCATTAAAGAAGTTGTC-3';
 PEP2 3' DCX, 5'-CGTCTAGATCAGCGAAATTTTTCAGG-3'.

Plasmids with inserts derived from PCR were completely sequenced. The corresponding fragments were cloned into PECE-FLAG or pGEX4T1.

Proteins

Recombinant DCX and mutated DCX were cloned in pRSET and transfected to *Escherichia coli* strain BL21, recombinant protein isolated on NiNTA columns according to the manufacturer's recommendations (Qiagen). Tubulin was

prepared from bovine brain extract as described (10). GST fusion peptide plasmids were transfected to *E.coli* strain BL21, and recombinant protein was isolated using glutathione-agarose beads (Sigma, Rehovot, Israel).

Antibodies

Anti- α tubulin (monoclonal, clone DM1A), or anti-acetylated tubulin (monoclonal, clone no. 6-11B-1) were purchased from Sigma. Anti-doublecortin polyclonal antibodies J74 were produced against a mixture of peptides (described in ref. 31).

Anti-FLAG M2 monoclonal antibodies

All secondary antibodies are from Jackson Immunoresearch (West Grove, PA): peroxidase-conjugated affinipure goat anti-mouse IgG (H+L), lissamine rhodamine-conjugated affinipure goat anti-mouse IgG (H+L), Cy3-conjugated affinipure goat anti-rabbit IgG (H+L), FITC-conjugated affinipure goat anti-mouse and anti-rabbit IgG (H+L).

GST pull-down assay

E18 brain extract or purified proteins were prepared in T-T buffer (20 mM Tris-HCl pH 8, 100 mM NaCl, 1 mM EDTA, 0.1% Triton-X), supplemented with protease inhibitors (Sigma). Proteins were incubated with 10 µg of GST-DCX, -PEP1, -PEP2, -PEP(1+2) and GST as control, at 4°C for 3–15 h. Glutathione beads (30 µl) in 300 µl of T-T buffer were added to the protein mixture and rotated for 30 min at room temperature. After four washes with T-T buffer, 2× sample buffer was added and the beads were boiled and ran on an SDS-PAGE gel. Western blot was performed with α -tubulin antibodies (monoclonal, clone DM1A).

Immunostaining

Briefly, transfected cells were plated on glass coverslips. After 48 h they were washed twice with phosphate-buffered saline (PBS), then fixed and permeabilized simultaneously in cold methanol for 10 min. After fixation the cells were incubated with 30 µl of the first antibody for 60 min at room temperature, then washed three times in PBS and incubated for 30 min with 30 µl of fluorescent-conjugated secondary antibodies. The coverslips were washed three times in PBS, drained and mounted. The immunostaining was visualized using an Olympus microscope (IX50 model; Hamburg, Germany) using the appropriate filters. Photography was with Kodak 160T film.

Detergent extraction assay

This was performed essentially as described by Cohen *et al.* (61) and Horesh *et al.* (33).

Microtubule assembly *in vitro*

Rate measurements. Tubulin was purified as described (10). The assembly rate of tubulin to form polymers was monitored using a light-scattering assay (62,63). Purified tubulin was diluted in PEM buffer (100 mM PIPES pH 6.9, 1 mM MgSO₄, 1 mM EGTA) supplemented with 1 mM GTP, to a final concentration of 16 µM. Recombinant proteins were dialyzed

against PEM buffer prior to their addition to the tubulin solution. Absorbance was measured at 350 nm at 1 min intervals in a uvicon spectrophotometer equipped with temperature-controlled cells. Switching the temperature to 37°C induced assembly.

Microscopy of microtubules. The effect of recombinant proteins on microtubule bundling was visualized by video-enhanced DIC microscopy. A solution (10 µl) containing phosphocellulose-purified tubulin and recombinant proteins, in PEM buffer supplemented with 1 mM GTP at indicated molar ratio was allowed to polymerize by incubation in an Eppendorf tube for 30 min at 26°C. A sample of the tube contents was transferred to microscope slides with coverslips mounted over parafilm spacers, and sealed with wax. DIC microscopy was performed using a Zeiss microscope equipped with a temperature-controlled oil immersion objective (Fluor 100/1.3).

Electron microscopy

Samples were prepared as described for DIC microscopy using tubulin at a concentration of 15 µM with or without the addition of 9 µM of *EcoRV* 1–213 fragment and incubated for 15 min at 37°C. Eight microliters of each sample was applied to a carbon-coated copper 400-mesh electron microscope grid, which had been previously glow-discharged to render the carbon surface hydrophilic. The grid was then rinsed with water, and 10 µl of uranyl acetate stain (1% in water) was applied. The grid was blotted after 30 s. Samples were examined with a Philips CM12 electron microscope operating at 100 kV.

ACKNOWLEDGEMENTS

This work was supported in part by the HFSP grant no. RG283199, Minerva Foundation, Germany, and the Minna James Heineman Foundation (to O.R.). O.R. is an incumbent of the Aser Rothstein Career Development Chair in Genetic Diseases. M.E. is an incumbent of the Delta Career Development Chair, and acknowledges support from the Israel Academy of Sciences and the Gerhard M.J. Schmidt Minerva Center for Supramolecular Architecture. S.P. acknowledges support from the Helen and Milton Kimmelman Center, supported by a research grant from the Kekst Family Center for Medical Genetics, the Forchheimer Center and the Crown Human Genome Center of the Weizmann Institute.

REFERENCES

- Aicardi, J. (1989) The lissencephaly syndromes. *Int. Pediatr.*, **4**, 118–126.
- Barth, P.G. (1987) Disorders of neuronal migration. *Can. J. Neurol. Sci.*, **14**, 1–16.
- Mischel, P., Nguyen, L. and Vinters, H. (1995) Cerebral cortical dysplasia associated with pediatric epilepsy. Review of neuropathologic features and proposal for a grading system. *J. Neuropathol. Exp. Neurol.*, **54**, 137–153.
- Barkovich, A.J., Kuzniecky, R.I., Dobyns, W.B., Jackson, G.D., Becker, L.E. and Evrard, P. (1996) A classification scheme for malformations of cortical development. *Neuropediatrics*, **27**, 59–63.
- Aicardi, J. (1991) The agyria–pachygyria complex: a spectrum of cortical malformations. *Brain Dev.*, **13**, 1–8.
- Kuchelmeister, K., Bergmann, M. and Gullotta, F. (1993) Neuropathology of lissencephalies. *Childs Nerv. Syst.*, **9**, 394–399.
- Reiner, O., Carrozzo, R., Shen, Y., Whener, M., Faustinella, F., Dobyns, W.B., Caskey, C.T. and Ledbetter, D.H. (1993) Isolation of a Miller–Dieker lissencephaly gene containing G protein β -subunit-like repeats. *Nature*, **364**, 717–721.
- Reiner, O. and Sapir, T. (1998) Abnormal cortical development; towards elucidation of the LIS1 gene product function. *Int. J. Mol. Med.*, **1**, 849–853.
- Lo Nigro, C.L., Chong, C.S., Smith, A.C., Dobyns, W.B., Carrozzo, R. and Ledbetter, D.H. (1997) Point mutations and an intragenic deletion in LIS1, the lissencephaly causative gene in isolated lissencephaly sequence and Miller–Dieker syndrome. *Hum. Mol. Genet.*, **6**, 157–164.
- Sapir, T., Elbaum, M. and Reiner, O. (1997) Reduction of microtubule catastrophe events by LIS1, platelet-activating factor acetylhydrolase subunit. *EMBO J.*, **16**, 6977–6984.
- Hattori, M., Adachi, H., Tsujimoto, M., Arai, N. and Inoue, K. (1994) Miller–Dieker lissencephaly gene encodes a subunit of brain platelet-activating factor. *Nature*, **370**, 216–218.
- Ross, M.E., Allen, K.M., Srivastava, A.K., Featherstone, T., Gleeson, J.G., Hirsch, B., Harding, B.N., Andermann, E., Abdullah, R., Berg, M. *et al.* (1997) Linkage and physical mapping of X-linked lissencephaly/SBH (XLIS): a gene causing neuronal migration defects in human brain. *Hum. Mol. Genet.*, **6**, 555–562.
- des Portes, V., Pinard, J.M., Smadja, D., Motte, J., Boespflug-Tanguy, O., Moutard, M.L., Desguerre, I., Billuart, P., Carrie, A., Bienvenu, T. *et al.* (1997) Dominant X linked subcortical laminar heterotopia and lissencephaly syndrome (XSCLH/LIS): evidence for the occurrence of mutation in males and mapping of a potential locus in Xq22. *J. Med. Genet.*, **34**, 177–183.
- des Portes, V., Pinard, J.M., Billuart, P., Vinet, M.C., Koulakoff, A., Carrie, A., Gelot, A., Dupuis, E., Motte, J., Berwald-Netter, Y. *et al.* (1998) A novel CNS gene required for neuronal migration and involved in X-linked subcortical laminar heterotopia and lissencephaly syndrome. *Cell*, **92**, 51–61.
- Gleeson, J.G., Allen, K.M., Fox, J.W., Lamperti, E.D., Berkovic, S., Scheffer, I., Cooper, E.C., Dobyns, W.B., Minnerath, S.R., Ross, M.E. and Walsh, C.A. (1998) *doublecortin*, a brain-specific gene mutated in human X-linked lissencephaly and double cortex syndrome, encodes a putative signaling protein. *Cell*, **92**, 63–72.
- Harding, B. (1996) Grey matter heterotopia. In Guerrini, R. (ed.), *Dysplasias of Cerebral Cortex and Epilepsy*. Lippincott-Raven, Philadelphia, PA, pp. 81–88.
- Barkovich, A.J., Guerrini, R., Battaglia, G., Kalifa, G., Nguyen, T., Parmeggiani, A., Santucci, M., Giovanardi-Rossi, P., Granata, T. and D'Incerti, L. (1994) Band heterotopia: correlation of outcome with magnetic resonance imaging parameters. *Ann. Neurol.*, **36**, 609–617.
- des Portes, V., Francis, F., Pinard, J.M., Desguerre, I., Moutard, M.L., Snoeck, L., Meiners, L.C., Capron, F., Cusmai, R., Ricci, S. *et al.* (1998) *doublecortin* is the major gene causing X-linked subcortical laminar heterotopia. *Hum. Mol. Genet.*, **7**, 1063–1070.
- Gleeson, J.G., Minnerath, S.R., Fox, J.W., Allen, K.M., Luo, R.F., Hong, S.E., Berg, M.J., Kuzniecky, R., Reitnauer, P.J., Borgatti, R. *et al.* (1999) Characterization of mutations in the gene *doublecortin* in patients with double cortex syndrome. *Ann. Neurol.*, **45**, 146–153.
- Kato, M., Kimura, T., Lin, C., Ito, A., Kodama, S., Morikawa, T., Soga, T. and Hayasaka, K. (1999) A novel mutation of the *doublecortin* gene in Japanese patients with X-linked lissencephaly and subcortical band heterotopia. *Hum. Genet.*, **104**, 341–344.
- Pilz, D.T., Matsumoto, N., Minnerath, S., Mills, P., Gleeson, J.G., Allen, K.M., Walsh, C.A., Barkovich, A.J., Dobyns, W.B., Ledbetter, D.H. and Ross, M.E. (1998) LIS1 and XLIS (DCX) mutations cause most classical lissencephaly, but different patterns of malformation. *Hum. Mol. Genet.*, **7**, 2029–2037.
- Pilz, D.T., Kuc, J., Matsumoto, N., Bodurtha, J., Bernadi, B., Tassinari, C.A., Dobyns, W.B. and Ledbetter, D.H. (1999) Subcortical band heterotopia in rare affected males can be caused by missense mutations in DCX (XLIS) or LIS1. *Hum. Mol. Genet.*, **8**, 1757–1760.
- Ohara, O., Nagase, T., Ishikawa, K., Nakajima, D., Ohira, M., Seki, N. and Nomura, N. (1997) Construction and characterization of human brain cDNA libraries suitable for analysis of cDNA clones encoding relatively large proteins. *DNA Res.*, **4**, 53–59.
- Nedivi, E., Hevroni, D., Naot, D., Israeli, D. and Citri, Y. (1993) Numerous candidate plasticity-related genes revealed by differential cDNA cloning. *Nature*, **363**, 718–722.
- Hevroni, D., Rattner, A., Bundman, M., Lederfein, D., Gabarah, A., Mangelus, M., Silverman, M.A., Kedar, H., Naor, C., Kornuc, M. *et al.*

- (1998) Hippocampal plasticity involves extensive gene induction and multiple cellular mechanisms. *J. Mol. Neurosci.*, **10**, 75–98.
26. Silverman, M.A., Benard, O., Jaaro, H., Rattner, A., Citri, Y. and Seger, R. (1999) CPG16, a novel protein serine/threonine kinase downstream of cAMP-dependent protein kinase. *J. Biol. Chem.*, **274**, 2631–2636.
 27. Vreugdenhil, E., Datson, N., Engels, B., de Jong, J., van Koningsbruggen, S., Schaaf, M. and de Kloet, E.R. (1999) Kainate-elicited seizures induce mRNA encoding a CaMK-related peptide: a putative modulator of kinase activity in rat hippocampus. *J. Neurobiol.*, **39**, 41–50.
 28. Burgess, H.A., Martinez, S. and Reiner, O. (1999) KIAA0369, Doublecortin-like kinase, is expressed during brain development. *J. Neurosci. Res.*, **58**, 567–575.
 29. Nagase, T., Ishikawa, K., Nakajima, D., Ohira, M., Seki, N., Miyajima, N., Tanaka, A., Kotani, H., Nomura, N. and Ohara, O. (1997) Prediction of the coding sequences of unidentified human genes. VII. The complete sequences of 100 new cDNA clones from brain which can code for large proteins *in vitro*. *DNA Res.*, **4**, 141–150.
 30. Matsumoto, N., Pilz, D.T. and Ledbetter, D.H. (1999) Genomic structure, chromosomal mapping, and expression pattern of human DCAMKL1 (KIAA0369), a homologue of DCX (XLIS). *Genomics*, **56**, 179–183.
 31. Francis, F., Koulakoff, A., Boucher, D., Chafey, P., Schaar, B., Vinet, M.C., Friocourt, G., McDonnell, N., Reiner, O., Kahn, A. *et al.* (1999) Doublecortin is a developmentally regulated, microtubule-associated protein expressed in migrating and differentiating neurons. *Neuron*, **23**, 247–256.
 32. Gleeson, J.G., Lin, P.T., Flanagan, L.A. and Walsh, C.A. (1999) Doublecortin is a microtubule-associated protein and is expressed widely by migrating neurons. *Neuron*, **23**, 257–271.
 33. Horesh, D., Sapir, T., Francis, F., Caspi, M., Grayer Wolf, S., Elbaum, M., Chelly, J. and Reiner, O. (1999) Doublecortin, a stabilizer of microtubules. *Hum. Mol. Genet.*, **8**, 1599–1610.
 34. Sullivan, L.S., Heckenlively, J.R., Bowne, S.J., Zuo, J., Hide, W.A., Gal, A., Denton, M., Inglehearn, C.F., Blanton, S.H. and Daiger, S.P. (1999) Mutations in a novel retina-specific gene cause autosomal dominant retinitis pigmentosa. *Nature Genet.*, **22**, 255–259.
 35. Lee, G., Neve, R.L. and Kosik, K.S. (1989) The microtubule binding domain of tau protein. *Neuron*, **2**, 1615–1624.
 36. Mandelkow, E. and Mandelkow, E.M. (1995) Microtubules and microtubule-associated proteins. *Curr. Opin. Cell Biol.*, **7**, 72–81.
 37. Maccioni, R.B. and Cambiasso, V. (1995) Role of microtubule-associated proteins in the control of microtubule assembly. *Physiol. Rev.*, **75**, 835–864.
 38. Ennulat, D.J., Liem, R.K., Hashim, G.A. and Shelanski, M.L. (1989) Two separate 18-amino acid domains of tau promote the polymerization of tubulin. *J. Biol. Chem.*, **264**, 5327–5330.
 39. Butner, K.A. and Kirschner, M.W. (1991) Tau protein binds to microtubules through a flexible array of distributed weak sites. *J. Biol. Chem.*, **115**, 717–730.
 40. Goode, B.L. and Feinstein, S.C. (1994) Identification of a novel microtubule binding and assembly domain in the developmentally regulated inter-repeat region of tau. *J. Cell Biol.*, **124**, 769–782.
 41. Lee, G. and Rook, S.L. (1992) Expression of tau protein in non-neuronal cells: microtubule binding and stabilization. *J. Cell Sci.*, **102**, 227–237.
 42. Preuss, U., Biernat, J., Mandelkow, E.M. and Mandelkow, E. (1997) The 'jaws' model of tau-microtubule interaction examined in CHO cells. *J. Cell Sci.*, **110**, 789–800.
 43. Goode, B.L., Denis, P.E., Panda, D., Radeke, M.J., Miller, H.P., Wilson, L. and Feinstein, S.C. (1997) Functional interactions between the proline-rich and repeat regions of tau enhanced microtubule binding and assembly. *Mol. Biol. Cell*, **8**, 353–365.
 44. Hutton, M., Lendon, C.L., Rizzu, P., Baker, M., Froelich, S., Houlden, H., Pickering-Brown, S., Chakraverty, S., Isaacs, A., Grover, A. *et al.* (1998) Association of missense and 5'-splice-site mutations in tau with the inherited dementia FTDP-17. *Nature*, **393**, 702–705.
 45. Hong, M., Zhukareva, V., Vogelsberg-Ragaglia, V., Wszolek, Z., Reed, L., Miller, B.I., Geschwind, D.H., Bird, T.D., McKeel, D., Goate, A. *et al.* (1998) Mutation-specific functional impairments in distinct tau isoforms of hereditary FTDP-17. *Science*, **282**, 1914–1917.
 46. Hasegawa, M., Smith, M.J. and Goedert, M. (1998) Tau proteins with FTDP-17 mutations have a reduced ability to promote microtubule assembly. *FEBS Lett.*, **437**, 207–210.
 47. Schweiger, S., Foerster, J., Lehmann, T., Suckow, V., Muller, Y.A., Walter, G., Davies, T., Porter, H., van Bokhoven, H., Lunt, P.W. *et al.* (1999) The Opitz syndrome gene product, MID1, associates with microtubules. *Proc. Natl Acad. Sci. USA*, **96**, 2794–2799.
 48. Cainarca, S., Messali, S., Ballabio, A. and Meroni, G. (1999) Functional characterization of the Opitz syndrome gene product (midin): evidence for homodimerization and association with microtubules throughout the cell cycle. *Hum. Mol. Genet.*, **8**, 1387–1396.
 49. Drewes, G., Ebneith, A., Preuss, U., Mandelkow, E.M. and Mandelkow, E. (1997) MARK, a novel family of protein kinases that phosphorylate microtubule-associated proteins and trigger microtubule disruption. *Cell*, **89**, 297–308.
 50. Altschul, S. and Gish, W. (1996) Local alignment statistics. In Doolittle, R. (ed.), *Methods in Enzymology*. Academic Press, New York, NY, pp. 460–480.
 51. Altschul, S.F., Madden, T.L., Schäffer, A.A., Zhang, J., Zhang, Z., Miller, W. and Lipman, D.J. (1997) Gapped BLAST and PSI-BLAST: a new generation of protein database search programs. *Nucleic Acids Res.*, **25**, 3389–3402.
 52. Henikoff, S., Henikoff, J.G., Alford, W.J. and Pietrokovski, S. (1995) Automated construction and graphical presentation of protein blocks from unaligned sequences. *Gene*, **163**, 17–26.
 53. Schuler, G.D., Altschul, S.F. and Lipman, D.J. (1991) A workbench for multiple alignment construction and analysis. *Protein Structure Function Genet.*, **9**, 180–190.
 54. Pietrokovski, S. (1994) Conserved sequence features of inteins (protein introns) and their use in identifying new inteins and related proteins. *Protein Sci.*, **3**, 2340–2350.
 55. Pietrokovski, S. (1998) Modular organization of inteins and C-terminal autocatalytic domains. *Protein Sci.*, **7**, 64–71.
 56. Pearson, W.R. (1995) Comparison of methods for searching protein sequence databases. *Protein Sci.*, **4**, 1145–1160.
 57. Metz, C.E. (1978) Basic principles of ROC analysis. *Sem. Nuclear Med.*, **8**, 283–298.
 58. Gluzman, Y. (1981) SV40-transformed simian cells support the replication of early SV40 mutants. *Cell*, **23**, 175–182.
 59. Ausubel, F.M., Brent, R., Kingston, R.E., Moore, D.D., Seidman, J.G., Smith, J.A. and Struhl, K. (1992) *Current Protocols in Molecular Biology 1*. Greene Publishing Associates and Wiley-Interscience, New York, NY.
 60. Deng, T. and Karin, M. (1993) JunB differs from c-Jun in its DNA-binding and dimerization domains, and represses c-Jun by formation of inactive heterodimers. *Genes Dev.*, **7**, 479–490.
 61. Cohen, O., Feinstein, E. and Kimchi, A. (1997) DAP-kinase is a Ca²⁺/calmodulin-dependent, cytoskeletal-associated protein kinase, with cell death-inducing functions that depend on its catalytic activity. *EMBO J.*, **16**, 998–1008.
 62. Herzog, W. and Weber, K. (1978) Fractionation of brain microtubule associated proteins. Isolation of two different proteins which stimulate tubulin polymerization *in vitro*. *Eur. J. Biochem.*, **92**, 1–8.
 63. Riederer, B., Cohen, R. and Matus, A. (1986) MAP5: a novel brain microtubule-associated protein under strong developmental regulation. *J. Neurocytol.*, **15**, 763–775.
 64. Schneider, T.D. and Stephens, R.M. (1990) Sequence logos: a new way to display consensus sequences. *Nucleic Acids Res.*, **18**, 6097–6100.